POAC'15
Trondheim, Norway

Proceedings of the 23rd International Conference on
Port and Ocean Engineering under Arctic Conditions
June 14-18, 2015
Trondheim, Norway

EXPERIMENTAL RELATIONSHIPS OF ARCTIC SEA ICE UNIAXIAL COMPRESSIVE STRENGTH WITH POROSITY

Zhijun Li [1], Qingkai Wang [1], Hongwei Han [1], Bingrui Li [2], Ruibo Lei [2]
[1] State Key Laboratory of Coastal and Offshore Engineering, Dalian University of Technology, Dalian, China
[2] China Polar Research Institute, Shanghai, China

ABSTRACT
During the Chinese Arctic Expedition in the summers of 2012 and 2014, the ice cores were taken at different ice camps in the higher latitude of Chukchi Sea or Beaufort Sea. The ice cores were then shipped to a cold room on RV Xuelong for ice compressive specimens. These specimens were used for the unconfined uniaxial compression tests which were performed for a wide range of displacement speed under temperature varying from −3°C to −9°C. Meanwhile, distributions of salinity, density, air content, fabric structure and grain size in vertical profiles in an ice sheet at each ice camp were examined. Thus, correlations between the uniaxial compressive strength and the porosity in ice specimens were studied. The compressive strength showed a non-linear relationship with the porosity, which was a function of ice temperature, salinity and density. The relationship is expected to develop a quantitative description about the variations of the mechanical behaviours with ice porosity or ice temperature, salinity and density under climate changes in Arctic summers.

INTRDUCTION
Recent years, the Arctic navigation in summer becomes warmly scientific and technical topics (Liu and Krobak, 2010; Shibata et al. 2013). Chinese had 6 times Arctic Science Expedition with RV Xuelong (Huang et al. 2013), the sea ice compressive strength experiments were started in the summer expedition in 2012 (Han et al. 2015) and 2014. For the ice service or ship design, the Chinese Arctic sea ice mechanical properties studies like a body. There is much space to fill in future. Also the ship design and ice service not only need ice compressive strength, but also ice flexure strength, elastic modulus, Poisson's ratio, ice-steel friction and so on (Tan et al. 2014; Kjerstad et al. 2015; Montewka, et al. 2015). Considering the first step on the ice mechanics in Chinese Arctic Scientific Expeditions, the uniaxial compressive strength is listed in the easily experimental studies because there are a longer history of ice compressive strength studies (Sinha, 1982; Timco and Frederking, 2010; Petrovic, 2003) and a lot of achievements and experiences in the world (Schwarz et al. 1981; Cole, 1987; Schulson, 2001; Moslet, 2007). The tensile strength, elastic modulus and fracture toughness are paying many efforts to obtain by using cleavage tests. The flexural strength and ice-steel friction are planned by comparing with Bohai sea ice system test results. This paper introduces the test technology and the fitted relations of the uniaxial compressive strength with strain rate and porosity. We expect using the specimen and test conditions to evaluate ice compressive strength with porosity and then use the field conditions to evaluate Arctic ice strengths with tested relations. Therefore, we expect using porosity (sea ice density, salinity and temperature) to connect the Arctic sea ice changes of "higher temperature" and lower

density under the global warming in summer time and expect extending the relationship to evaluate sea ice other mechanical properties with porosity under climate changes.

SAMPLING AND TEST TECHNOLOGY

In order to study the regional differences in the uniaxial compressive properties of the sea ice, specimens for mechanical testing were sampled with a Kovacs drill (Kovacs Enterprise, Roseburg, OR, USA) with a corer 9 cm in diameter at each of ice camp. The specimens were collected as full-length ice cores. Its in-situ temperature and salinity measurements were obtained from one core, and another core was used for density measurements and crystal structure analysis. The temperature of the sea ice was measured immediately after the ice core was removed from the ice cover. A Pt100 needle probe with an accuracy of ±0.1°C was used to measure the temperature in holes drilled into the side of the core at 5 cm intervals. Following this, the core was cut lengthwise to obtain vertical sections 5–10 cm thick and sealed in plastic boxes, to be used for the salinity measurements. The salinity was measured with an SYA2-2 salinometer with a precision of 0.005‰ after the ice samples were melted. Other ice cores were taken, labeled and stored in a cold laboratory (−15°C) on board the RV Xuelong. In the cold laboratory, the density and crystal core was cut lengthwise to obtain vertical sections 5–10 cm thick for density measurements and crystal structure analysis. The density of the ice was measured using a volume method. After the density measurements, the thick vertical sections were cut into two layers with a sawing machine for crystal structure analysis. The vertical sections were cut to a thickness of 0.5–0.2 mm and placed on a universal stage to observe the crystal structure between crossed polarizing filters.

Based on the crystal structure analysis, the ice compressive test specimens with 9 cm in diameter in cross section and about 20 cm in length were cut from these compressive cores by bone saw. These specimens were cut from the transition layer and the columnar ice layer; the thin granular ice layer at the top of the ice core was cut off. Therefore, the compressive tests need many ice cores. Total 140 ice cores were taken and their total length was 196 m in 2012, and total 62 ice cores were taken and their total length was 84 m in 2014. The positions of the ice camps in 2012 and 2014 are listed in Table 1 and Figure 1.

Table 1. The ice camps information and ice conditions.

Summer	Camp	Date	Longitude	Latitude	Ice thickness /cm	Free board /cm	Snow thickness /cm
2012	1#	29 Aug.	120°28.248′E	86°47.987′N	113	7	11
	2#	30 Aug.	123°04.857′E	87°39.640′N	140	12	15
	3#	31 Aug.	120°19.154′E	86°36.955′N	77	3	17
	4#	1 Sept.	145°15.114′E	84°59.952′N	199	12	20
	5#	1 Sept.	158°48.070′E	84°05.711′N	128	8	13
	6#	1 Sept.	161°43.070′E	83°37.650′N	178	12	9
2014	A#	10 Aug.	151°03.876′W	76°42.953′N	174	17	7
	B#	11 Aug.	154°35.570′W	77°10.984′N	107	14	5
	C#	13 Aug.	163°07.948′W	77°29.269′N	200	12	11
	D#	14 Aug.	160°57.513′W	78°16.460′N	122	12	7
	E#	16 Aug.	158°36.724′W	79°55.793′N	140	12	7
	F#	17-26 Aug.	157°35.454′W	80°51.290′N	135	10	8
	G#	28 Aug.	152°38.2869′W	79°58.6123′N	100	6	2.7
	H#	28 Aug.	149°21.5854′W	78°48.3752′N	114	13	14

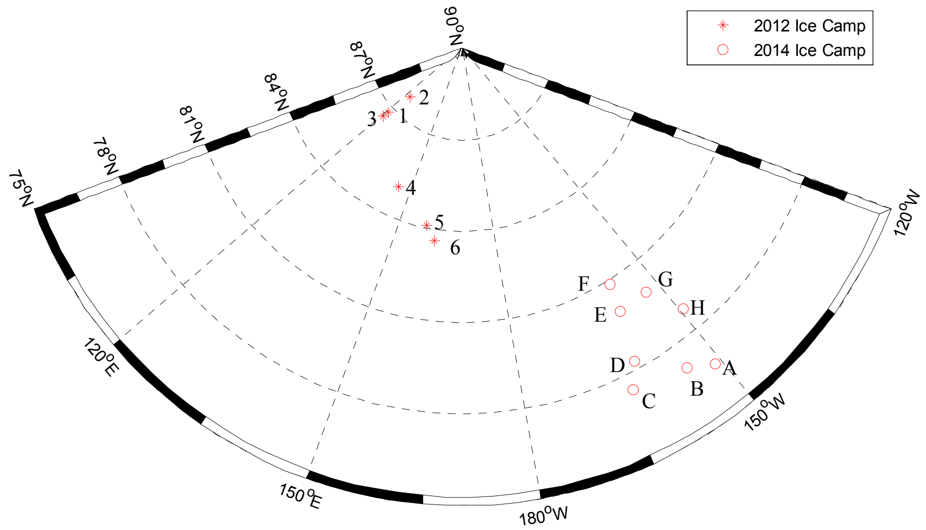

Figure 1. Ice camps in the 2012 (No. 1 to No.6) and 2014 (No. A to No. H) CHINARE Arctic Expeditions.

After the suggestions on ice mechanical properties tests (Schwarz et al. 1981), the tested specimen size in 2012 was not follow the standard size, then a modified lathe for ice specimen with 7.0 cm in diameter and 17.5 cm in length was used in 2014. Considering thermal equilibration process of ice specimen, the specimen was put into a low-temperature cabinet with a precision of 0.1°C, and the storage time was over 24 h to ensure that the inside and outside of the specimen had a consistent temperature before the test.

The upper platen of the testing machine was attached to a hydraulic actuator (100 kN capacity) to provide pressure for the tests. A PPM226-LS2-1 load sensor was used to measure the force; the maximum capacity of this sensor was 50 kN, with a linearity of 0.2%. An LM10 micro-laser sensor was used to measure the deflection of the loading point. The range of measurement was 130 mm, the linearity was 0.2%, and the resolution was 0.02 mm. Figure 2 gives the test equipments.


Figure 2. Compressive strength test equipments.

TEST RESULTS

The tests were performed in two summers. Except the porosity effects, train rate effect is quite important, therefore, the tests used different displacement speed (see Table 2). Arctic sea ice crystal is complex and tested specimen has some special broken style. But most of them are similar with thermal growth sea ice. Figure 3 is the normal case of ice specimen broken and special phenomenon. These ductile or brittle broken forms change with temperature and strain rate. All of them can be found from literature studies (see Figure 3a and 3b). The Arctic summer sea ice sometimes is with clear refrozen hard layers and soft layers and lager channels or bubbles, the specimen was displaced under compression and the stress-strain curve was special phenomenon (see Figure 3c).

Table 2. Sea ice compressive strength in 2012 and 2014.

Summer`	Ice camp	−3℃	−6℃	−9℃	Test aims for different effects
2012	1#	✓			Density
	2#	✓	✓	✓	Temperature and Strain rate
	3#	✓	✓	✓	Temperature and Strain rate
	4#	✓	✓	✓	Temperature and Strain rate
	5#	✓			Specimen size
	6#	✓	✓	✓	Temperature and Strain rate
2014	A#	✓			Strain rate
	C#		✓		Strain rate
	F#	✓	✓	✓	Temperature and Strain rate
	G#		✓		Strain rate

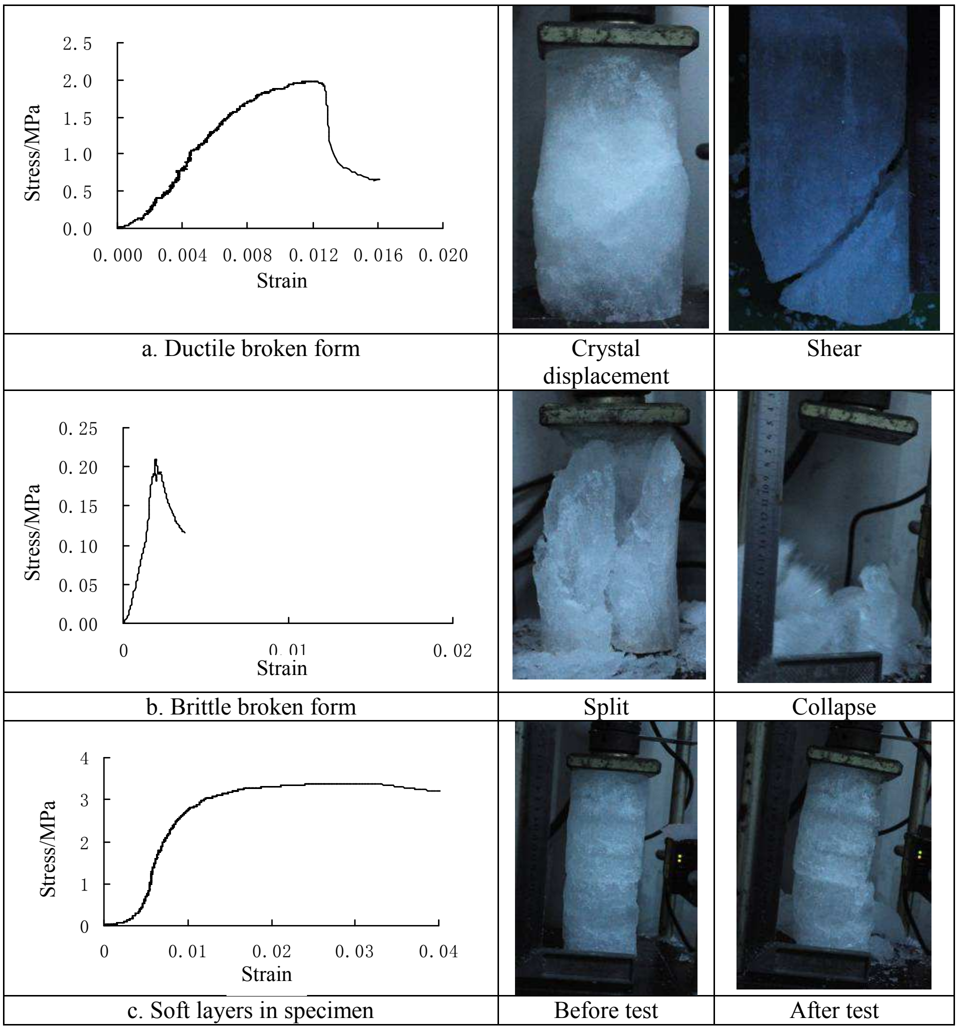

Figure 3. Arctic sea ice compressive broken stress-strain curves and broken phenomenon.

As shown in literatures on ice compressive strength (Sinha, 1982; Cole, 1987), each test can have a stress with a certain stress rate or train rate. In the curve pf lg-lg between the strength and stress rate or strain rate, a group of tested strength at same temperature can be shown. On the results in 2012, the curve with stress rate was used because one of the laser sensors worked partly. Most ice crystal was columnar ice except the specimens from Ice camp at −3 °C. Therefore the compressive strength is similar with the results of sea ice compression along the direction vertical with ice surface. Figure 4 gives one of the curves.

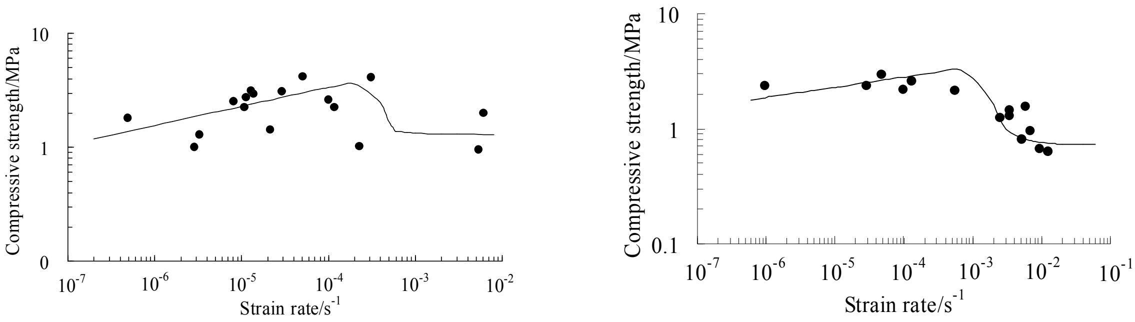

(a) 2012 (b) 2014

Figure 4. Uniaxial compressive strength of Arctic summer sea ice from Ice camp 3 tested at −6°C in 2012 and Ice camp C tested at −6°C in 2014.

In spite of the shortage of strain rate in the measurement in 2012, the strain rate can be connected with floating ice speed in the calculation of ice forces on vertical structures, therefore, the data set of ice compressive strength, strain rate and calculated porosity by Cox and Weeks (1983) is set up. Based on the data set, the relationship between the strength, strain rate and porosity is obtained by statistical method, see Figure 5. This relation is similar with Bohai sea ice compressive strength (Li et al. 2011). Comparing with Bohai test results, the Arctic sea ice data is much scatter because Arctic ice fabric structure is more complex with mixture of grain crystal, columnar crystal, frozen blocks, etc.

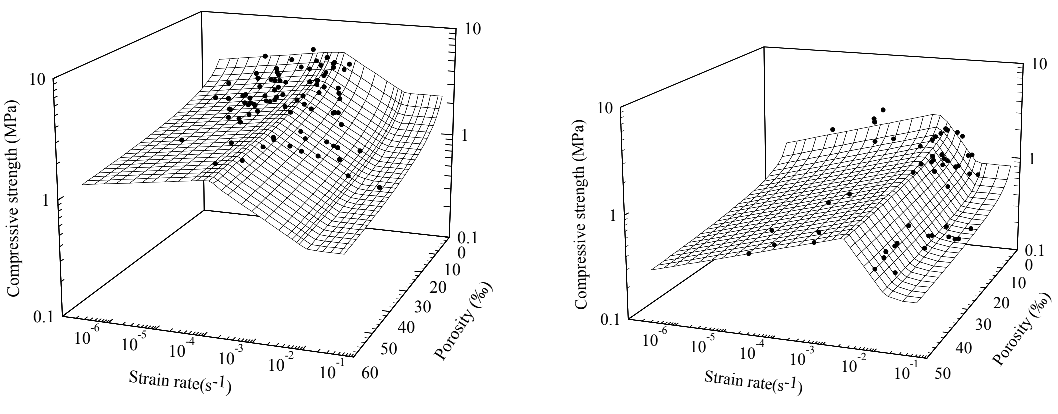

(a) 2012 (b) 2014

Figure 5. Relation between compressive strength, strain rate and porosity from 2012 tests.

DISCUSSIONS ON THE USEAGE OF THE TEST RESULTS

With the Arctic warming, the sea ice temperature becomes higher and near the phase change point, so the ice density and porosity become more sensitive parameter. Especially the density should be considered in future research. Therefore the density measurement also become more and more popular measured data (Timco and Frederking, 1996). If the density is one of the measured data, the ice mechanical evaluation can use porosity (function of ice temperature, salinity and density) instead of brine volume in ice (function of ice temperature and salinity). We try to used the test results from ice specimen to ice sheet by using Timco and Frederking (1990)'s method. In fact, the summer Arctic sea ice temperature is near melting point, therefore the porosity is evaluated by Cox and Weeks (1983)'s formulas in test conditions, and the porosity in Arctic summer conditions sometimes need to use Leppäranta and Manninen (1988)'s formula because the higher ice temperature.

The strain rate or stress rate corresponding the peak strength in Figure 4 is changes with temperature, therefore the peak position on the strain rate in Figure 5 is not a constant. The temperature is lower the peak position of strain rate smaller. The peak strength value is a useful index for ice resistance design, and it can be evaluated with ice temperature because the value is sensitive with temperature even porosity is more accurate. In 1980-90's, the peak strength-ice temperature is important evaluation relation. Table 3 summaries the data from 2012.

Table 3 The tested ice temperature and peak compressive strength

Ice camp	Latitude/°	Tested ice temperature/°C	Peak compressive strength/kPa
1#	86.79978	−3	2.90
2#	87.66067	−3	4.30
		−6	5.30
		−9	5.76
3#	86.61592	−3	2.85
		−6	3.45
		−9	3.27
4#	84.99920	−3	2.85
		−6	4.12
		−9	3.46
5#	84.09518	−3	2.78
6#	83.62750	−3	2.89
		−6	3.76
		−9	3.99

Using the data in Table 3, Figure 6 is made. This relation between the peak strength and ice temperature is non-linear and considering the fact that ice freezing point temperature is different from ice melting point temperature. While sea water is frozen, the freezing point changes with salinity and pressure, it can be expressed with a formula (Foldvik and Kvinge, 1974). While sea ice melting, the brine inside ice will be become liquid from solid first, the corresponding temperature depends on the brine salinity. The brine salinity is higher than sea water salinity, therefore the high brine ice start change phase at lower temperature than that of sea water freezing point temperature. After the high brine ice change phase, the brine channels become wider and wider, the ice bearing capability becomes lower and lower, but it does not reach to 0 at sea water freezing point temperature because most part of sea ice is pure ice crystals. These crystals are melted around 0 °C. Therefore, there are two different curves for the peak strength vs. ice temperature, one is for ice forming process and one is for ice melting process. Because the analysis above has not data to support, here the melting point without strength is supposed as −0.3 °C with 0.1 MPa.

Figure 6 is the basement of design peak compressive strength. Following the measured ice temperatures meet in the route of 2012 and the ice core temperatures, the lowest ice temperature −1.75 °C is assumed as the design ice temperature. From Figure 6 and Figure 7, the design Arctic summer ice compressive strength is 2.12 MPa at lower latitude (dotted line in Figure 6) and 3.17 MPa at higher latitude (solid line in Figure 6 and data around 88° latitute).

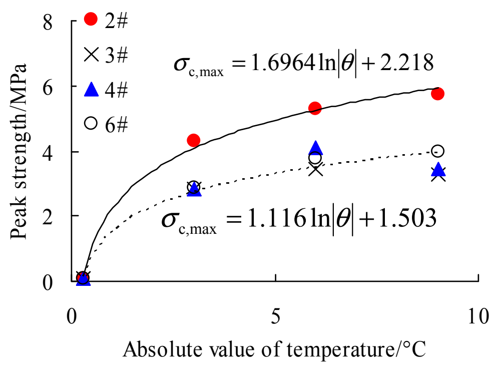

Figure 6. The peak strength vs. ice temperature in 2012.

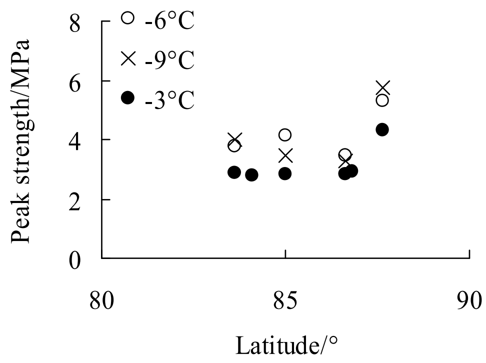

Figure 7. The peak compressive strength with latitude in the summer of 2012.

CONCLUSIONS

The most compression broken phenomenon of Arctic summer sea ice are similar with that of simple crystal sea ice. Because there are some complex fabrics in Arctic due to the dynamic or multi-year ice, some displacement phenomenon and special curve of stress-strain occurred in Arctic sea ice.

There is the relation between compressive strength and strain rate, porosity for Arctic summer ice. Comparing with the statistical result of Bohai ice, the strength data are more scatter.

The design peak compressive strength for ice resistance structures can be evaluated by using traditional relation between the peak strength and ice temperature. Based on the tested data in 2012, the design ice temperature in the summer of 2012 is −7.5 °C and the corresponding design peak compressive strength is 2.12MPa at latitude lower than 88° and 3.17MPa at latitude higher 88°.

ACKNOWLEDGMENTS

We sincerely thank the crew of the RV Xuelong for providing excellent logistic supports. The Fifth and Sixth Chinese National Arctic Research Expeditions in 2012 and 2014 were organized by the Chinese Arctic and Antarctic Administration. The fieldwork was supported by the Polar Research Institute of China. After the expedition, the data analysis and research were supported continuously by National Basic Research Program of China (973 Program) (No.2015CB953901) and National Natural Science Foundation of China (41376186). We also try to transfer the understandings to Arctic navigation in summer under the support of High Technology of Ship Research Project of the Ministry of Industry and Information Technology (2013417-01). Parts of international cooperation actions are supported by International Science and Technology Cooperation Program of China (2011DFA22260), Public Science and Technology Research Funds Projects of Ocean (201205007-05).

REFERENCES

Cole, D. M., 1987. Strain rate and grain size effects in ice. Journal of Glaciology, 33(115): 274-280.

Cox, G. F. N., Weeks, W. F., 1983. Equations for determining the gas and brine volumes in sea-ice samples. Journal of Glaciology, 29: 306-316.

Foldvik, A. and Kvinge, T., Conditional instability of sea water at the freezing point. Deep Sea Research and Oceanographic Abstracts, 1974, 21(3):169-174.

Han, H., Li, Z., Huang, W., et al., 2015. The uniaxial compressive strength of the Arctic summer sea ice. Acta Oceanologica Sinica, 34(1):129-136.

Huang, W., Lei, R., Ilkka, M., et al., 2013. The physical structures of snow and sea ice in the Arctic section of 150°-180° W during the summer of 2010. Acta Oceanologica Sinica, 32(5): 57-67.

Kjerstad, Ø. K., Metrikin, I., Løset, S., et al., 2015. Experimental and phenomenological investigation of dynamic positioning in managed ice. Cold Regions Science and Technology, 111: 67-79.

Leppäranta, M., Manninen, T., 1988. The brine and gas content of sea ice with attention to low salinities and high temperatures. Internal Rep 88–2, Helsinki: Finnish Institute for Marine Research.

Li, Z., Zhang, L., Lu, P., et al., 2011. Experimental study on the effect of porosity on the uniaxial compressive strength of sea ice in Bohai Sea. Science China-Technical Science, 54(9):2429-2436.

Liu, M. J. and Kronbak, J., 2010. The potential economic viability of using the Northern Sea Route (NSR) as an alternative route between Asia and Europe. Journal of Transport Geography, 18(3):434-444.

Montewka, J., Goerlandt, F., Kujala, P., et al., 2015. Towards probabilistic models for the prediction of a ship performance in dynamic ice. Cold Regions Science and Technology, 112: 14-28.

Moslet, P. O., 2007. Field testing of uniaxial compression strength of columnar sea ice. Cold Regions Science and Technology, 48: 1-14.

Petrovic, J. J., 2003. Review mechanical properties of ice and snow. Journal of Materials Science, 38(1):1-6.

Schulson, E, M., 2001. Brittle failure of ice. Engineering Fracture Mechanics, 68(17):1839-1887.

Schwarz, J., Frederking, R. M. W., Gavrillo, V., et al., 1981. Standardized testing methods for measuring mechanical properties of ice. Cold Regions Science and Technology, 4: 245-253.

Shibata, H., Izumiyama, K., Tateyama, K., et al., 2013. Sea-ice coverage variability on the Northern Sea Routes, 1980–2011. Annals of Glaciology, 54(62):139-148.

Sinha, N. K., 1982. Constant strain and stress-rate compressive strength of columnar-grained ice. Journal of Materials Science, 17(3): 785-802.

Tan, X., Riska, K., Moan, T., 2014. Effect of dynamic bending of level ice on ship's continuous-mode icebreaking. Cold Regions Science and Technology, 106-107: 82-95.

Timco, G. W. and Frederking, R. M. W., 1990. Compressive strength of sea ice sheets. Cold Regions Science and Technology, 17(3): 227-240.

Timco, G. W. and Frederking, R. M. W., 1996. A review of sea ice density. Cold Regions Science and Technology, 24(1):1-6.

Timco, G. W., Weeks, W. F., 2010. A review of the engineering properties of sea ice. Cold Regions Science and Technology, 60:107-129.